SENSORLESS SPEED CONTROL OF A SWITCHED RELUCTANCE MOTOR FOR INDUSTRIAL APPLICATIONS

J. Wolff R. Rahner H. Späth
Elektrotechnisches Institut, Universität Karlsruhe
Kaiserstraße 12, 76128 Karlsruhe, Germany
Email: wolfju@eti.etec.uni-karlsruhe.de

Abstract: *The Elektrotechnische Institut of the University Karlsruhe has developed, optimised and manufactured a Switched Reluctance Drive with power converters and control engineering according to the latest scientific findings. The motor has been constructed for the rated output power of 18,5kW at 1500r.p.m. for industrial applications. The common supply for the voltage-source converter is 3x400V/50Hz. For this application the authors have developed a method to estimate the rotor position and the speed without a rotor position encoder. This method calculates the position of the rotor by using the flux linkage and the phase currents of the motor.*

Keywords: *OPTIM,* Switched Reluctance Motor, Sensorless Speed Control, Estimation of Rotor Position

1. Introduction

The sensorless speed control and the estimation of the rotor position have already been treated in several publications. The authors of these publications preferrably used smaller motors or high-speed drives for their tests. (e.g. [Brö] 2Nm/1200r.p.m., [Lyo] 34Nm/25.000r.p.m.)
Differing from these publications, this paper will discuss the sensorless speed control of a motor with a relatively high rated torque of 118 Nm. Furthermore, the strength of this Switched Reluctance Motor must be seen in a speed range below 1000r.p.m. Within this range, its efficiency and its dynamic is very high [Wo1].
This paper treats the operation of a high torque SR-drive for low-speed applications without a rotor position encoder.
The results of this test do not provide a complete solution for the sensorless speed control but they can be seen as basic idea and as stimulation for following further tests. The selection of the method, its restrictions and possibilities will be discussed here.

2. Motor design

The Elektrotechnische Institut selected the Switched Reluctance Motor with 16 stator poles and 12 rotor teeth. It is a 4-phase-winding machine, the 4 stator poles that are shifted by 90° to each other form one phase-winding (Figure 1).

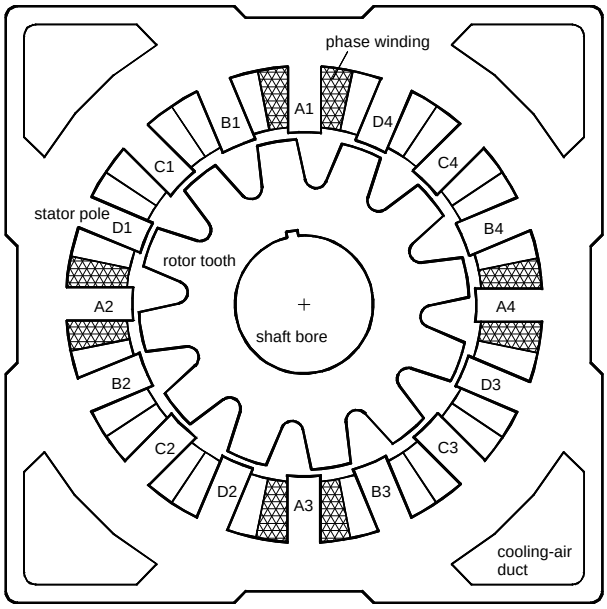

Figure 1: Schematic cross-section of the Switched Reluctance Motor

3. Voltage-source converter

The voltage-source converter consists of a mains and a motor converter. The common supply for the three-phase-self-commutated mains converter is 400V/50Hz. The d.c. link voltage U_d is constantly set to 750V. Figure 2 shows the circuit of the load-side converter.

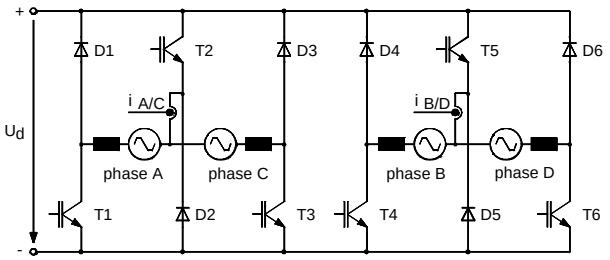

Figure 2: Circuit of the load-side converter

The phases A and C respectively B and D should not conduct current at the same time, since for example A generates a motor- and C a generator-torque. Both torques are subtracted from each other, a not desirable status. Therefore, the phases A and C respectively B and D can be supplied with one common transistor without further restrictions regarding the current control. The currents can be determined by one common measurement.

4. Flux-current method

The procedure for the sensorless estimation of rotor position and speed must be suitable for the test drive with 18,5kW, 118Nm and 1500r.p.m. It definitely has to use the non-linear model of the Switched Reluctance Motor. A very good overview of sensorless methods for determining the rotor position of switched reluctance motors is given in [Ray]. For the test drive, we selected the flux-current method.

Before being produced the 16/12 Switched Reluctance Motor was optimised and calculated with a finite element method (Figure 3).

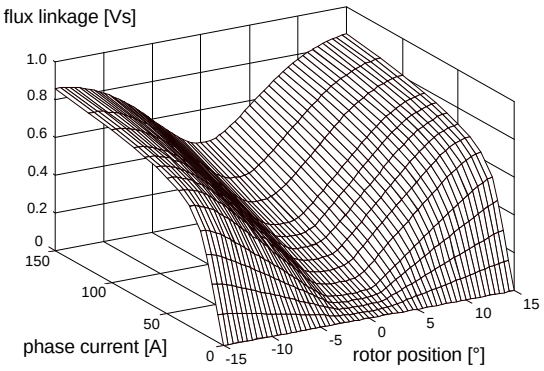

Figure 3: Characteristic of flux linkage depending on current and rotor angle (calculation)

Figure 3 shows the flux linkage for a rotor position between -15° and 15°. The value +/- 15° is the aligned position. Stator pole and rotor tooth are in line, 0° is the unaligned position. At this position, there is a gap between the teeth opposite to the stator pole. The motor has 12 rotor teeth and so this characteristic feature is repeated for the observed stator pole respectively for the observed phase 12 times per rotation. Furthermore, the reference field is symmetrical between 0° to 15° and 0° to -15°. One rotor rotation corresponds to 360°.
With the known phase current and flux linkage, the rotor position can be read out of this characteristic. This is the basic idea of the flux-current method.
The successful use of this method basically depends on the accuracy of the calculated characteristic. Since the flux linkage had not been measured for the test motor a comparison is not possible.
However, the torque depending on the rotor position and phase current was calculated for the torque control by means of this characteristic. The following equations were used:

$$W^* = \int_0^i y \; di \qquad \text{(eq. 1)}$$

$$m = \frac{d\ W^*}{d\ j} \qquad \text{(eq. 2)}$$

Figure 4 illustrates the very good correspondence between calculation and actual measurement results.

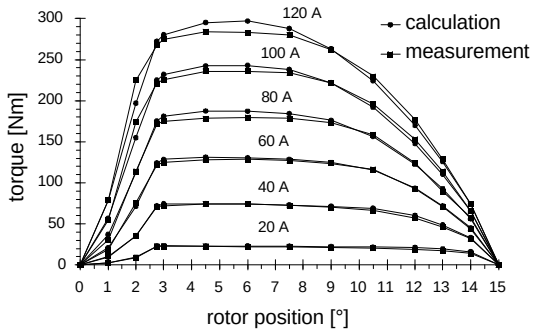

Figure 4: Torque depending on rotor position with phase current as parameter (comparison of measurement and calculation)

The various torque testings were performed using a locked rotor with the phase current as parameter. The rotor position was varied. Since the measured torque corresponded very well to the torque calculated by means of the flux linkage, we assumed that the characteristic of the calculated flux linkage would also correspond to the actual values and would therefore be suitable for the flux-current method.

In order to be able to read the rotor position out of the characteristic (figure 3), the flux-linkage needs to be defined.
The electrical part of the SRM can be described by the voltage equation of the machine:

$$u = R \cdot i + \frac{d\ y\ (i, j\ )}{d\ t} \qquad \text{(eq. 3)}$$

In this equation u means the phase voltage, R the coil resistance and ψ the flux linkage.

To calculate the mechanical rotor position, the current and the flux linkage must be given. It is not difficult to define the current since we can use the measurement of the normal motor-control. It is, however, much more complicated to define the present flux linkage in the machine. We calculate the flux by eq. 4, a special form of the voltage-equation.

$$y = \int (u - R \cdot i)\, dt \qquad \text{(eq. 4)}$$

This algorithm has been realised by a small analogue-circuitry, in discrete technology (Figure 5). Main component of this hardware application is the integrator which can be controlled and reset with the help of a finite state machine.

The gate switch impulses (T1 to T6) for the power transistors constitute the inputs for the circuit. These impulses are generated by the current controllers realised by means of analogue circuits.

The current controllers are two-step controllers, Further inputs are the current measurement values $i_{A/C}$ and $i_{B/D}$.

The three-phase-self-commutated mains converter sets the d.c. link voltage in steady operation to constant 750V. Even during a higher load change and transient reactions this voltage remains within a tolerance band of 730V to 770V [Wo2]. This allows to use the gate switch impulses of the transistors to determine the phase voltage u. Due to the circuit of the load-side converter the phase voltage can be -750V (i>0), 0V or +750V.

The phase voltage is determined by means of a logic using the levels of the gate switch impulses. If the d.c. link voltage is not stable, the actual measurement value would additionally have to be considered in this logic.

In the next step, the ohmic voltage drop above the phase resistance is deducted from the phase voltage. It is calculated by multiplying the measured current value with the phase resistance. The phase resistance is 110mΩ given a winding temperature of 20°C. With a continuous running duty in the rated point, it increases to approximately 155mΩ. The amplitude of the phase current is approximately 60A at the rated torque. Like this, the amplitude of the ohmic voltage drop is between 6V and 9,3V. Compared to the phase voltage, this value is very small and could therefore possibly be neglected. Since the calculation of the ohmic voltage drop could easily be realised, it was taken into consideration. The following integrator integrates this voltage difference up to the flux linkage. The value of the flux linkage and also the value of the phase current are transmitted via A/D converters to the digital signal processor for further processing.

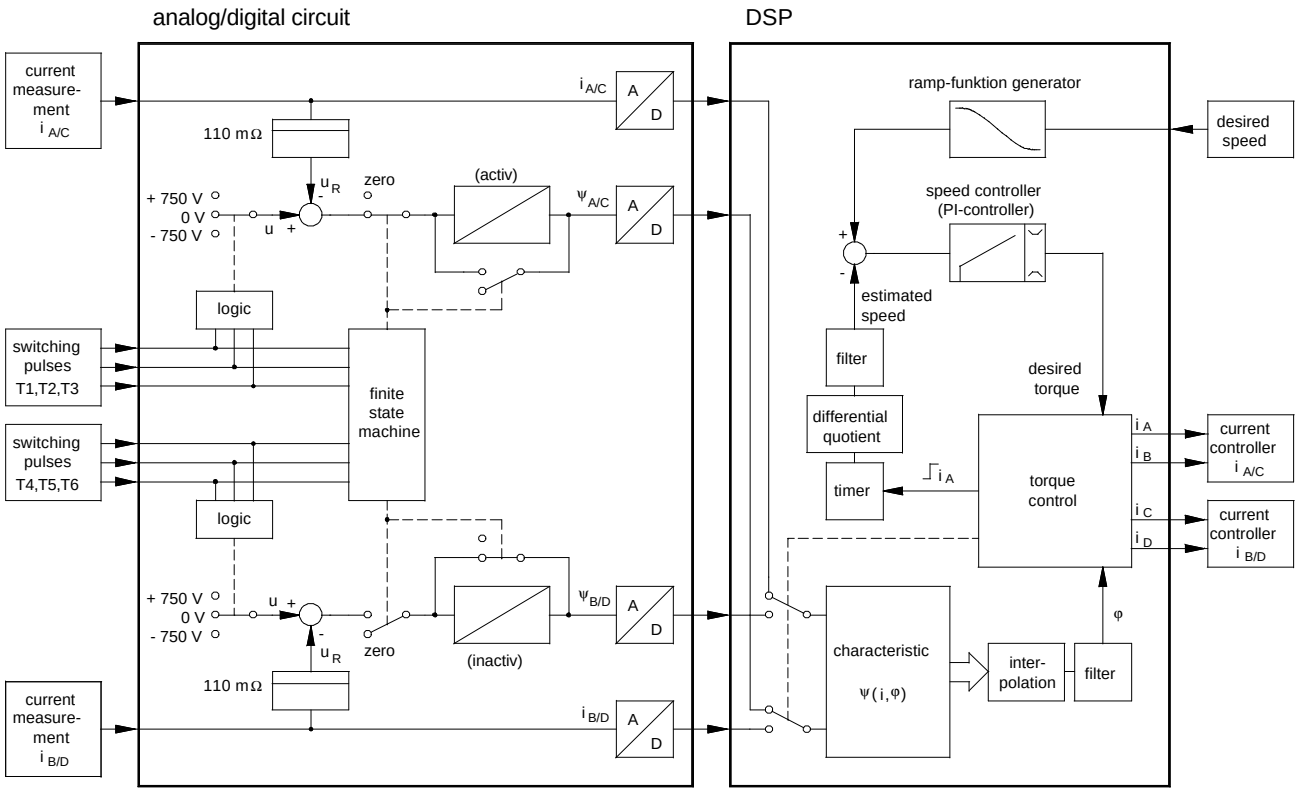

Figure 5: Realisation and implementation of the flux-current method

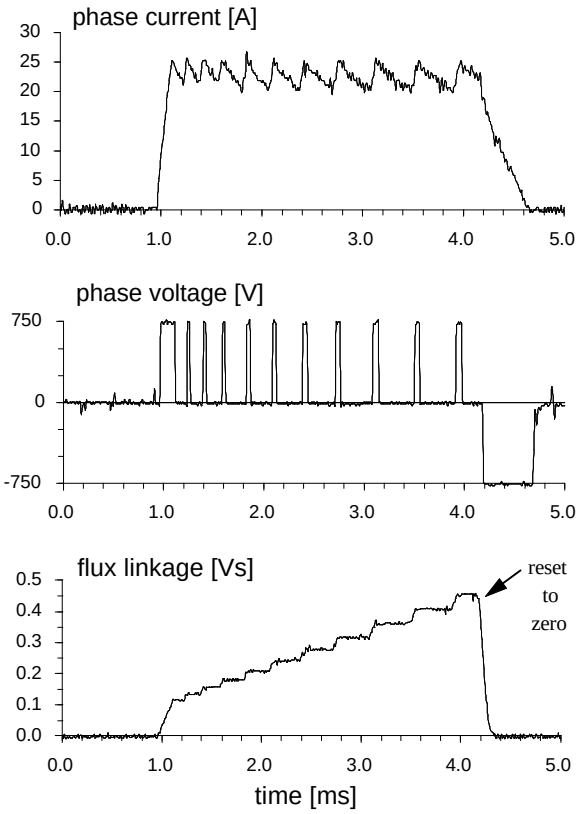

Figure 6: Phase current, phase voltage and flux-linkage at 30Nm and 400r.p.m. (measurement)

For calculating the flux linkage only two integrators are needed for four motor phases. Similar to only one current measurement needed for 2 phases, the flux linkage of 2 phases can be calculated with one integrator. The integrator interval for one phase begins with the rising edge of the phase current and ends with the current rising edge of the next phase. During one integration interval the rotor turns by 7,5°. A finite state machine determines the beginning and the end of the integration intervals from the switch impulses. At the end of an interval the output of the integrators is set back to zero by an electronic switch. It remains zero until a new integration interval begins.

A part of the characteristic according to figure 3 for the rotor position from 0° to 15° was saved to the memory of the DSP (Digital Signal Processor). Due to the symmetry already described this is sufficient for defining the angle. We used TMS320C40 from Texas Instruments as DSP. The sampling time is 120 µs. In the beginning of each detection cycle the analogue current controllers receive the new aim values. Afterwards the actual measurement values of the phase currents and the values of the flux-linkage are read in. For the value of the flux linkage and the respective measurement value of the current, the required pairs of interpolation points are read out of the characteristic in the DSP memory. This is used to define the rotor angle by means of an interpolation.

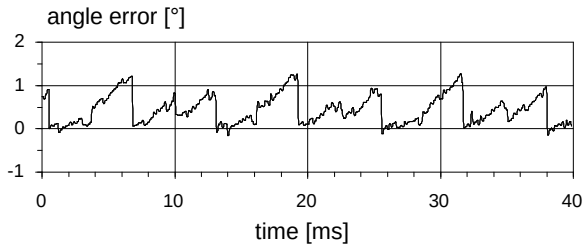

Figure 7: Difference between estimated and original rotorposition at 30Nm and 400r.p.m. (measurement)

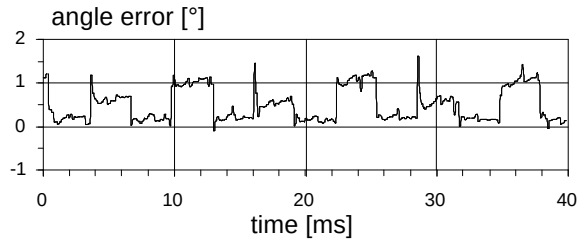

Figure 8: Difference between estimated and original rotorposition at 120Nm and 400r.p.m. (measurement)

As an example, figures 7 and 8 illustrate the error of the angle estimation for two operation points of the switched reluctance motor. The error is the difference between the estimated rotor position and the values measured by a rotor position encoder. It ranges between 0,5° and 1,5° (mechanical angle). The evident jumps allow to allocate the error values to the single integration intervals. An integration interval corresponds to a rotor rotation of approximately 7,5°. At a speed of 400r.p.m. the rotor rotates by 7,5° in 3,12ms.

5. Iron loss

With higher speeds the angle error increased noticeably towards the end of the 7,5° interval. The estimated angle is smaller than the actual rotor position. According to the model shown in figure 9 the measured phase current is devided into two currents.

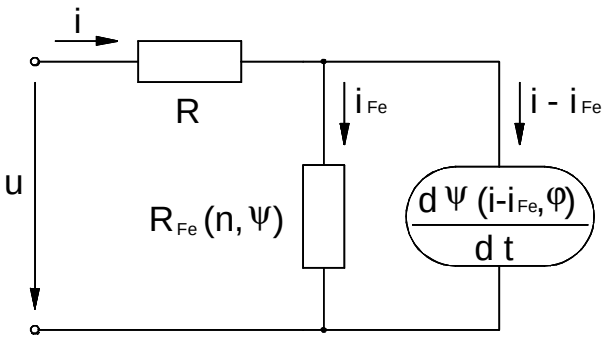

Figure 9: Substitutional block diagram of a phase under consideration of iron losses

The first partial current i_{Fe} covers the iron losses of the switched reluctance machine. It flows via the resistance R_{Fe}. Only the second partial current $i-i_{Fe}$

influences the flux linkage value as magnetising current. According to the characteristic in figure 3 the flux linkage is only known with dependency on the magnetising current and the rotor angle. Therefore, the measured phase current must be reduced by i_{Fe} for reading the rotor position out of the reference field. For the test drive, i_{Fe} was calculated using equation 5:

$$i_{Fe} = const. \cdot n \cdot y^{2} \cdot i \qquad \text{(eq. 5)}$$

This estimation allowed to expand the sensorless speed control to a speed of 1.200r.p.m. The constant was determined in an experimental way.
In figures 7 and 8 the correction according to equation 5 was already taken into consideration.

6. Angle filter

Despite the good results for the estimation of the rotor position, single values can vary strongly from the actual position. There are ranges within the characteristic of the flux-linkage where smaller changes of the current or flux cause a bigger change of the rotor position. Within these ranges, already smaller measurement inaccuracies cause a relatively big error in the estimation of the rotor position. Experiments have shown that the estimation within an angle ranging from -3° to -7° respectively from 3° to 7° operates very reliably. For the remaining range the estimated angle should undergo a plausibility check. Due to the inertia moment of the motor, the speed remains almost constant during a sampling time of 120µs. If the angle of the actual sampling instant which is estimated from the flux linkage deviates from the previous detection step in inadmissable size, the new angle is calculated by the previous angle and product of speed and sampling time.
Within the torque control the estimated angle is required for defining the switch-on / switch-off times for the phase currents. Torque and speed control of the Switched Reluctance Drives are described in [Wo1]. They have also been implemented on the DSP.

7. Speed estimation

It is necessary to determine the actual speed value for the speed control. This is done by means of the timewise change of the estimated angle. A timer in the DSP determines the time period needed for at rotor revolution of 30°. Within the angle interval of 30° (π/6) each of the 4 phases is activated once. Beginning and ending of a phase are defined by the beginning current increase in phase A. The moving average value above three of such angle intervals is the actual speed for the comparison of actual and aim values of the speed controller (eq. 6).

$$n = \frac{1}{2p} \cdot \frac{1}{3} \sum_{k=1}^{3} \frac{p/6}{\Delta t(k-3)} \qquad \text{(eq. 6)}$$

The differential quotient of angle change

$$n = \frac{1}{2p} \frac{\Delta j}{T_A} \qquad \text{(eq. 7)}$$

and detection period did - even with afterwards filtering not provide a useable result. For this difference quotient the fluctuations of the angle estimation are to strong.

8. Dynamic running

In addition to the stationary running a dynamic running must also be possible. After a load change the speed control should quickly reset the actual speed to the aim value. Furthermore the actual speed should quickly follow after a change of the aim value. Within stationary running aim and actual value must correspond to each other.
Figure 10 shows a load jump from 20Nm to 120Nm at 500r.p.m., produced by a DC-motor, which is coupled to the Switched Reluctance Motor. The dynamic of the sensorless speed control is, in this case, relatively good. After approximately 400ms the actual speed reaches the aim value again. The use of single speed measurement with a rotor position encoder did not provide better results [Spä].

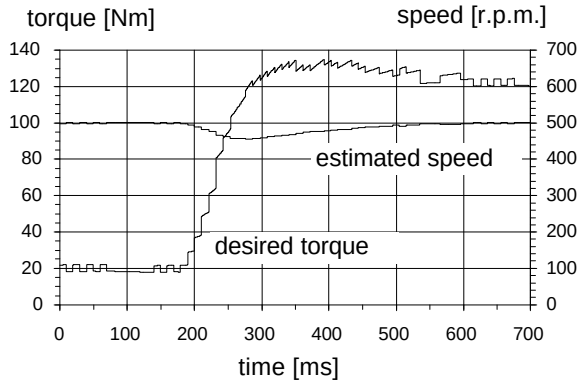

Figure 10: Load jump from 20Nm to 120Nm at 500r.p.m. sensorless, J_{all} = 0,54kgm^2 (measurment)

Figure 11 shows the speed course after a jump of the aim value form 400r.p.m. to 1000r.p.m. The sensorless speed control needs a relatively long period for these interim processes.
A ramp function generator restricts the aim value jumps to an admissible ramp before aim and actual values are compared. When the slope of this ramp increases noticeably the motor will pull out of synchronism.

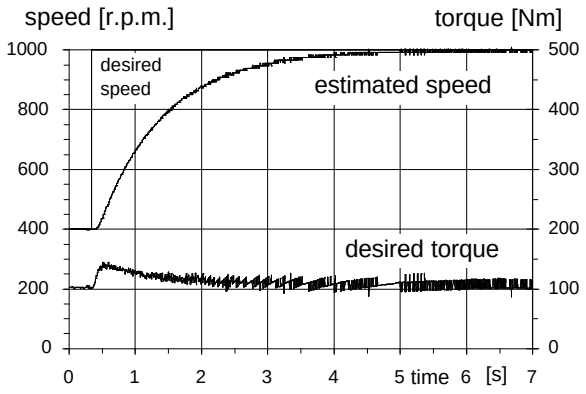

Figure 11: Speed jump from 400r.p.m. to 1000r.p.m. at a load of about 100Nm sensorless, J_{all} = 0,54kgm^2 (measurment)

In stationary running the correspondence of aim and actual values is widely safeguarded (figures 10, 11).
The reason for the unsteady running of the estimated speed and also of the desired torque must be seen in the speed calculation. Only after a rotation of 30° a new speed value is calculated. During these angle intervals, the value of the estimated speed remains constant.

9. Conclusion

The flux-current method allowed to realise the sensorless speed control within a speed range of 200r.p.m. to 1200r.p.m. up to 150Nm for the test drive. The sensorless control allows load jumps and variable speeds.
Given the characteristic of the flux linkage, this procedure can easily be realised.
The operation below 200r.p.m would either call for an improved voltage integration or for a different method. A speed higher than 1200r.p.m. requires a more accurate estimation of the iron loss.
The filtering of the estimated values has to be seen as a basic problem.

10. Acknowledgements

Optimisation and calculation of the Switched Reluctance Motor were made by Mr E. Vonhof at Power Electronics Dublin using a Finite Elemente Program. We thank the Deutsche Forschungs-gemeinschaft for its financial support of this research project.

Symbols

i	phase current
i_{Fe}	current for the iron losses
i_A	current of the phase A (A/B/C/D phase quantities)
J	moment of inertia
m	phase torque
n	motor speed
R	winding resistance
R_{Fe}	resistance for the iron losses
t	time
T_A	sampling time
u	phase voltage
U_d	d.c. link voltage
W*	coenergy
φ	rotor position (mechanical angle)
ψ	flux linkage

converter features

typ	IGBT double-way converter (laboratory converter)
supply connection	3x400V, 50Hz
max. mains load	40kW
mains power factor	≅ 1
d.c. link voltage	750V

motor features

typ	MFR 132.5
manufacturer	Elbtalwerk Heidenau GmbH
rated output	18,5kW
rated torque	118Nm
rated speed	1500r.p.m.
duty type	continuous running (S1)
thermal class	F
shaft heigh	132mm
moment of inertia	0,0883kgm^2

11. References

[Brö] Brösse, A.; Henneberger, G.: Sensorless Control of a Switched Reluctance Motor Using a Kalman Filter. Proceedings of the 7th European Conference on Power Electronics and Applications, Vol. 4, p. 561-566, Trondheim 1997

[Lyo] Lyons, J.P.; MacMinn, S.R.; Preston, M.A.: Flux/Current Methods For SRM Rotor Position Estimation. IEEE IAS Conf., p. 482-487, 1991

[Wo1] Wolff, J.; Späth, H.: Switched Reluctance Motor with 16 stator poles and 12 rotor teeth. Proceedings of the 7th European Conference on Power Electronics and Applications, Vol. 3, p. 558-563, Trondheim 1997

[Ray] Ray, W.F.; Al-Bahadly, I.H.: Sensorless Methods for Determining the Rotor Position of Switched Reluctance Motors. Proceedings of the EPE, p. 7-12, Brighton 1993

[Ste] Steiert, U.: Drehmomentsteuerung einer Reluktanzmaschine mit beidseitig ausgeprägten Polen und geringer Drehmomentwelligkeit. Dissertation Universität Karlsruhe, 1992

[Wo2] Wolff, J.; Bauer, G.; Simon, O.: Netzfreundlicher Anschluß elektrischer Antriebe an das Drehstromnetz durch verbesserte Regelung. atp (1997) No. 11, p. 44-51

[Spä] Späth, H.; Wolff, J.: Der elektrische Antrieb der Zukunft? TECHNIKA (1996) No. 19, p. 49-53